EuroIntervention 2016;12:e605-e614 published online e-edition August 2016

Early coverage of drug-eluting stents analysed by optical coherence tomography: evidence of the impact of stent apposition and strut characteristics on the neointimal healing process

Renick Lee[1], BEng; Nicolas Foin[1,2]*, MSc, PhD; Jaryl Ng[1], BEng; John Allen[1,2], PhD; Nicole Soh[1,2], BEng; Ivy Ang[3], BEng; Winston Shim[1,2,3], PhD; Ryo Torii[4], MSc, PhD; Philip Wong[1,2,3], MD

1. National Heart Centre Singapore, Singapore; 2. Duke-NUS Medical School, Singapore; 3. Innoheart Plc, Singapore, Singapore; 4. University College London, London, United Kingdom

KEYWORDS

- blood flow
- coverage
- drug-eluting stent (DES)
- malapposition
- re-endothelialisation
- strut thickness

Abstract

Aims: Previous studies have associated issues such as incomplete stent apposition with delayed healing and adverse events (stent thrombosis). The aim of this study was to evaluate the impact of strut apposition and stent type on the progression of stent strut coverage.

Methods and results: We evaluated *in vivo* in porcine models the follow-up response and coverage characteristics of well-apposed and malapposed segments of drug-eluting stents (DES) (CYPHER, PROMUS Element and Orsiro) and the Absorb bioresorbable vascular scaffold (BVS) by optical coherence tomography (OCT) sequentially, at baseline, and at one week and four weeks of follow-up. Supporting results were provided by histological analysis performed at four-week follow-up and computer simulation describing the shear characteristics around apposed and non-apposed struts. A total of 325 cross-sections containing 3,166 struts were analysed. The extent of malapposition decreased over time as a result of neointimal healing (from 7.1% at baseline to 0% at four weeks; p=0.03). At one week, 13.6% of struts in well-apposed segments were still uncovered versus 19.2% of struts in malapposed cross-sections and 77.8% of NASB struts (p<0.01). At four-week follow-up, 3.1% of struts were uncovered in well-apposed cross-sections vs. 1.6% in malapposed cross-sections and 35.7% of NASB struts (p<0.01). A comparison of the apposed segments revealed that the thin-strut Orsiro had only 1.3% of uncovered struts at one week while PROMUS Element, CYPHER and BVS had 6.6%, 48.4% and 16.2% of struts still uncovered, respectively.

Conclusions: This study shows that early coverage is influenced by stent apposition as well as platform strut characteristics (stent type). At four weeks, NASB struts remained a focus of delayed endothelialisation.

**Corresponding author: National Heart Centre Singapore, 5 Hospital Drive, Singapore 169609, Singapore. E-mail: nicolas.foin@nhcs.com.sg*

© Europa Digital & Publishing 2016. All rights reserved.

SUBMITTED ON 02/12/2015 - REVISION RECEIVED ON N/A - ACCEPTED ON 09/12/2015

DOI: 10.4244/EIJV12I5A100

Introduction

Incomplete stent apposition (ISA) is defined as the separation of at least one stent strut from the vessel wall. Various studies have associated stent malapposition with poor healing results, incomplete endothelialisation, fibrin deposits and stent thrombosis[1-4]. Coverage and ISA have been suggested as potential underlying risk factors in stent thrombosis and, while their impacts are still unclear, intravascular imaging studies show that ISA is often associated with delayed strut coverage[1,5-8].

Neointimal healing starts immediately after stent implantation and can rectify acute malapposition[1,9,10]. There is much value in assessing re-endothelialisation and coverage because of their association with the prevention of adverse outcomes such as late stent thrombosis, as illustrated by pathological[11] and imaging studies[9] ascertaining neointimal coverage. Factors leading to either good integration or delayed coverage of stent segments left unapposed during implantation are, however, still not completely understood.

Intravascular imaging such as optical coherence tomography (OCT) or intravascular ultrasound (IVUS) are used to guide procedures and assess optimal stent expansion. In practice, however, when ISA is detected by IVUS or OCT, there is currently no guideline available for clinicians on when further optimisation is necessary or what degree of prosthesis underexpansion may lead to complications.

Preclinical animal studies are generally based on well-deployed stents and delayed coverage is rarely observed. However, absence of coverage remains an important issue for patients, and delayed coverage can be observed long after implantation, as shown by intravascular imaging and pathological studies[2,6,9,11-13].

To study the impact of strut apposition on the neointimal healing process, we evaluated in a controlled animal *in vivo* environment the early coverage trends of well-apposed versus malapposed struts at successive follow-up time points.

Methods

STUDY SAMPLES

Four stent types were used in this study, namely three drug-eluting stents (DES), CYPHER® (Cordis, Johnson & Johnson, Warren, NJ, USA, n=2), PROMUS Element™ (Boston Scientific, Marlborough, MA, USA, n=4) and Orsiro (Biotronik AG, Bulach, Switzerland, n=3), and the Absorb bioresorbable vascular scaffold (BVS 1.1) (Abbott Vascular, Santa Clara, CA, USA, n=5). CYPHER has a strut thickness of 140 µm, a polyethylene co-vinyl acetate/poly-n-butyl methacrylate (PEVA/PBMA) permanent polymer with coating thickness of 12.6 µm, and contains the drug sirolimus[14]. PROMUS Element has an 81 µm strut thickness with a permanent fluorinated durable polymer and everolimus coating. Orsiro has a 60 µm strut thickness, a bioabsorbable poly-L-lactic acid (PLLA) with silicon carbide layer and conformable sirolimus biodegradable coating[14]. BVS is a polylactic acid (PLA)-based everolimus-eluting scaffold consisting of a PLLA backbone with a 1:1 copolymer poly(DL-lactide) (PDLLA) drug surface coating and has a strut thickness of 156 µm[14]. The stents were implanted in the coronary vessels of six porcine models and deployed in tapered left anterior descending (LAD), left circumflex (LCX) and right coronary artery (RCA) vessel segments. The stents (2.5-3.5 mm in diameter, 18-28 mm in length) were post-dilated using delivery balloons to achieve a stent-to-artery ratio of 1.1-1.2 in the 2/3 most distal part of the stents, leaving the proximal edges of the stents incompletely apposed.

IMPLANTATION AND FOLLOW-UP TIME POINTS

Quantitative coronary analysis (QCA) was performed on the pre-implant angiogram to identify carefully an appropriate target site for stent implantation. Stents were deployed across the side branch without ensuring full expansion of the segment proximal to the side branch. This was achieved by first expanding the stents to their nominal pressures (~7 atm), then advancing the balloon distally to full pressure (~12 atm).

The study involved analyses of the OCT images obtained from the vessels of the pigs at baseline, and at one-week and four-week follow-up. Thirty-seven OCT pullbacks were obtained using LightLab Dragonfly™ OCT imaging catheters (St. Jude Medical, St. Paul, MN, USA) (out of 42 planned OCT, five pullbacks could not be acquired because the OCT catheter could not be re-crossed into the stent). Contiguous cross-sections at 2 mm intervals in the stented segments were analysed.

Strut apposition was assessed on each analysed cross-section and then averaged per stent. Struts were determined as being malapposed when the distance between the middle of the strut's reflective surface (metal) and the vessel wall was larger than the sum total of the strut and polymer thickness. Non-apposed side branch (NASB) struts were defined as struts floating at the ostium of side branches with no vessel wall and were treated as a separate classification from the ISA segments[15].

A strut was defined as uncovered when no visible tissue was observed covering the endoluminal strut side[16]. Neointimal coverage thickness was defined/measured as in previous studies by taking the distance from the edge of the strut boundary (reflective surface) to the neointima-lumen interface measured along a straight line from the longitudinal axis midpoint to the vessel centreline[15].

For BVS, a threshold for coverage of 30 µm was used from the edge of the strut "black box" to take into account the polymer strut contour, as previously shown[17]. Frames containing ISA/NASB struts at baseline were matched to corresponding frames at follow-up.

HISTOLOGICAL PROCESSING

At four weeks, the stented vessel segments were fixed in 10% formalin, dehydrated in a graded series of ethanol and embedded in methyl methacrylate plastic. After polymerisation, sections of 200 µm were sawed from each stented artery. Sections from the stents were mounted, stained with methylene blue and further thinned using milling and polishing. Re-endothelialisation, restenosis and intimal inflammation were assessed as previously described. A total of 33 histological cross-sections were used for the histology analysis.

COMPUTATIONAL SIMULATION

Simulation of flow was conducted to describe the shear profile in the case of jailed side branch (struts) by quantifying the spatial means of time (cycle) averaged endothelial shear stress (TAESS) on the luminal side of the struts in the ostium region, as well as proximal and distal to the ostium.

STATISTICAL ANALYSIS

All strut-related variables were evaluated first across each particular stent with each stent used as an independent unit of clustering. The average measure of strut coverage and coverage thickness was used for each individual stent at a given time point. Results were analysed and presented as previously recommended for analysis of clustered OCT data[18]. Strut malapposition and strut coverage were expressed as percentages of uncovered strut and percentage of malapposed struts.

Percentage of uncovered strut, percentage of malapposed struts, and average coverage thickness were compared among stent types using mixed model analysis of variance with animals as a random effect, and stent type, time (weeks one, four) and stent type×time interaction as fixed effects **(Table 1)**. Similarly, coverage thickness and percentage of uncovered strut were compared among well-apposed, malapposed and NASB segment treatment groups using mixed model analysis of variance. In both analyses, selected *post hoc* pairwise comparisons were performed on group×time interaction least-squares means. P-values <0.05 were considered statistically significant.

Results

OCT COVERAGE ANALYSIS

A total of 37 OCT pullbacks were performed (14 stents×3 time points=42; five pullbacks were unobtainable and excluded from the study). Out of the 37 acquired and analysed pullbacks, 28 pullbacks contained ISA and/or NASB struts. Analysis of the progression of coverage on well-apposed struts showed an increase in the mean coverage thickness **(Figure 1)**. Overall, strut malapposition decreased over time from 7.1% at baseline to 1.3% at one week and 0% at four weeks **(Figure 2)**.

IMPACT OF STRUT APPOSITION

At one-week follow-up, strut coverage was 86.4% in well-apposed segments versus 80.8% in malapposed cross-sections and only 22.2% in NASB struts (p<0.01). At four-week follow-up, strut coverage was 96.9% and 98.4% in well-apposed and malapposed sections, respectively, as compared to 64.3% of NASB struts **(Figure 3A, Figure 3B)**. Coverage at follow-up was found on average to be thickest on apposed struts (0.02 mm at one week, 0.12 mm at four weeks) followed by malapposed struts (0.05 mm at one week, 0.11 mm at four weeks) and least on NASB struts (0.01 mm at one week, 0.03 mm at four weeks) **(Figure 3A, Figure 3C)**.

IMPACT OF STENT TYPE

The influence of stent type on coverage was analysed by comparing results of well-apposed sections across the three different stent types (CYPHER, PROMUS Element, Orsiro) **(Figure 4, Table 2)**. At one week, the rate of uncovered strut was highest in CYPHER (48.4%) followed by BVS (16.2%) and PROMUS Element (6.6%), and least in Orsiro (1.3%) **(Figure 4)**. At four weeks, all well-apposed segments were covered except in BVS (0.6%) and Orsiro (0.2%). Orsiro displayed the greatest mean coverage thickness (0.14 mm) at four weeks followed by CYPHER (0.13 mm) and BVS (0.13 mm), with the lowest being in PROMUS Element (0.12 mm).

Table 1. Percentage malapposition.

S/N	Pig	Stent	Baseline			1 week			4 weeks		
			Malapposed	Apposed	% Malapposed	Malapposed	Apposed	% Malapposed	Malapposed	Apposed	% Malapposed
1	1	PROMUS	3	91	4.2	0	70	0	0	48	0
2	1	Orsiro	29	52	35.8	0	99	0	0	21	0
3	2	PROMUS	16	68	14.7	0	50	0	0	57	0
4	2	CYPHER	4	65	3.7	0	75	0	0	92	0
5	2	Orsiro	5	133	4.5	0	153	0	0	170	0
6	3	PROMUS	10	73	13.5	19	78	16.6	0	43	0
7	3	Orsiro	0	117	0.0	0	115	0	0	112	0
8	4	BVS	3	71	6.3	0	65	0	0	57	0
9	4	BVS	0	62	0.0	0	60	0	0	71	0
10	4	CYPHER	0	62	0.0	0	90	0	0	76	0
11	5	BVS	4	106	2.2	0	83	0	–	–	–
12	5	BVS	–	–	–	0	109	0	–	–	–
13	6	BVS	0	99	0.0	0	104	0	–	–	–
Average% Malapposed			7.1			1.3			0.0		
SD			10.3			4.6			0.0		

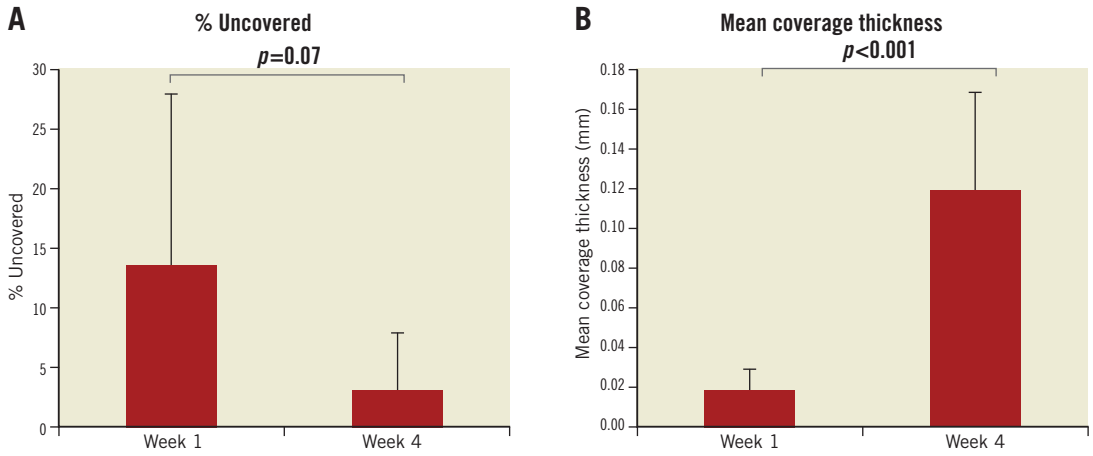

Figure 1. *Evolution of strut coverage with follow-up time. A) Percentage of struts uncovered from well-apposed stent struts at one-week and four-week follow-up. B) Corresponding mean strut coverage thickness at one-week and four-week follow-up.*

HISTOLOGICAL ANALYSIS

All stents performed similarly with regard to vascular characteristics according to histological analysis at four weeks post stenting of the coronary vessels in the animals examined **(Figure 5A)**. Neointimal areas were on average similar for CYPHER (1.1 mm^2), PROMUS Element (1.4 mm^2) and Orsiro (1.2 mm^2), but comparatively higher in BVS (1.9 mm^2, p<0.001) **(Figure 5B)**. The inflammation scores of the vessels examined were similar (1 vs. 0.9 vs.

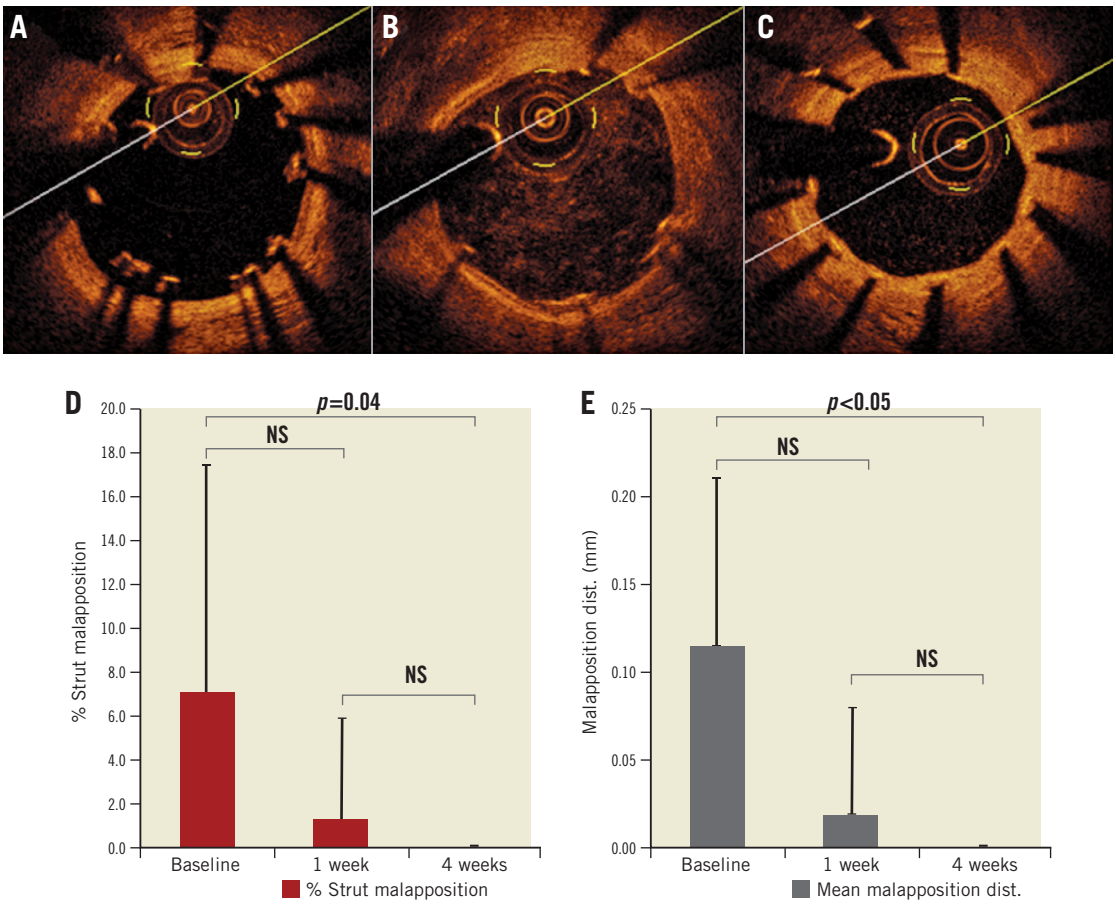

Figure 2. *Evolution of incomplete strut apposition over time. OCT images of malapposed struts. A) Baseline. B) One-week follow-up. C) Four-week follow-up. D) Proportion of struts malapposed by percentage at baseline, one-week and four-week follow-up. E) Mean malapposition distance (the distance between the middle of the strut's reflective surface and the vessel wall) of malapposed struts from the wall at baseline, one-week and four-week follow-up.*

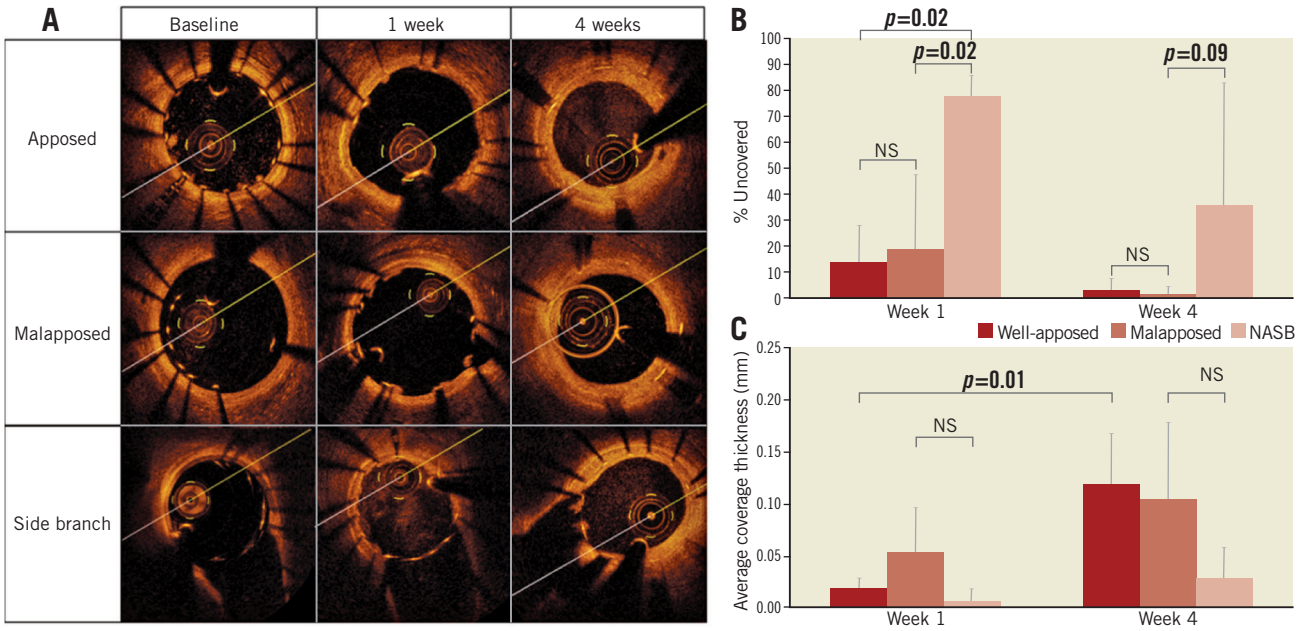

Figure 3. *Strut coverage depending on apposition. A) OCT images showing coverage of apposed, malapposed and NASB struts at baseline, one-week and four-week follow-up. B) Proportion of struts uncovered by percentage in apposed, malapposed and NASB cases at one-week and four-week follow-up. C) Mean neointimal coverage thickness of apposed, malapposed and NASB struts at one-week and four-week follow-up.*

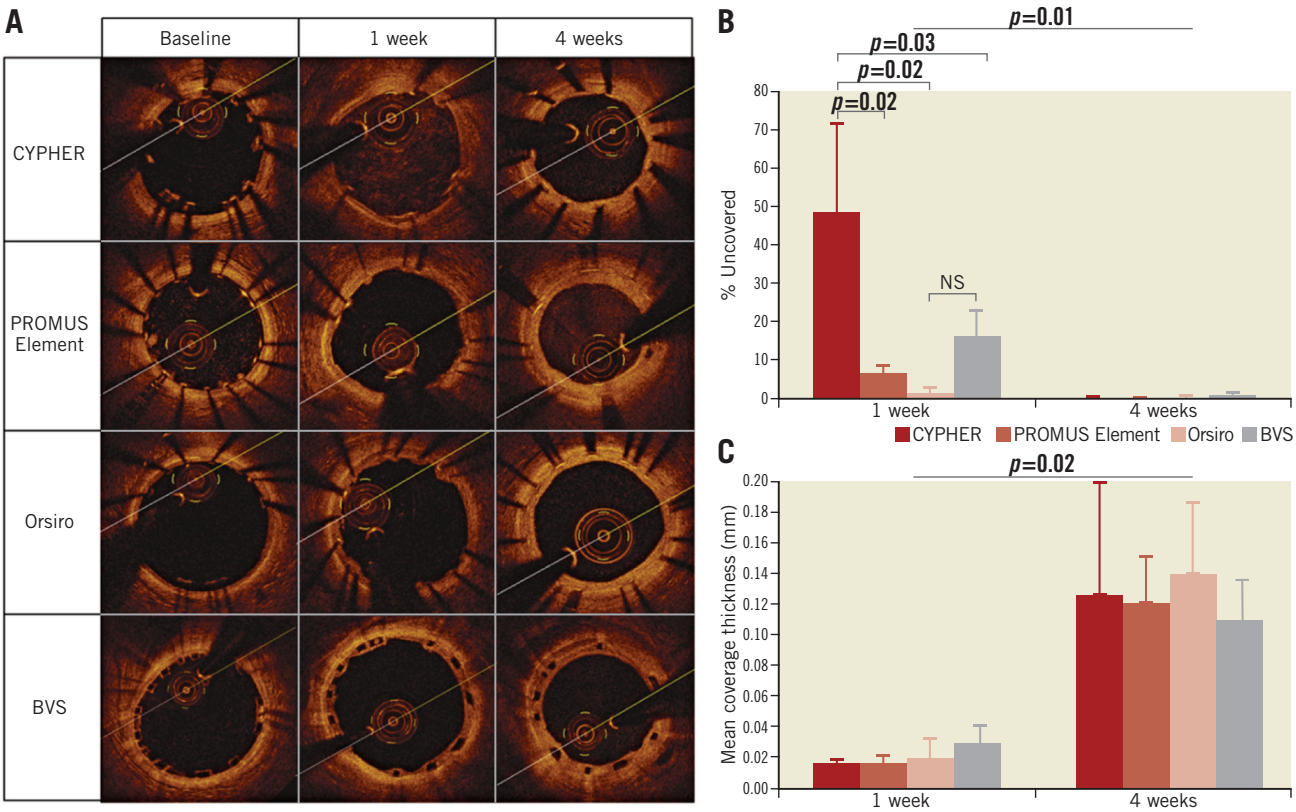

Figure 4. *Strut coverage evolution for different stent designs: CYPHER, PROMUS Element, Orsiro and BVS. A) OCT images showing coverage of stent struts at baseline, one-week and four-week follow-up. B) Proportion of struts uncovered by percentage of stents at one-week and four-week follow-up. C) Mean coverage thickness of stent struts at one-week and four-week follow-up.*

Table 2. Coverage on apposed segment.

S/N	Pig	Stent	1 week			4 weeks		
			Uncovered	Covered	% uncovered	Uncovered	Covered	% uncovered
1	1	PROMUS	5	55	7.4	0	50	0
2	1	Orsiro	1	98	1.0	0	22	0
3	2	PROMUS	3	38	8.2	0	37	0
4	2	CYPHER	24	51	31.9	0	81	0
5	2	Orsiro	5	151	2.7	1	170	0.6
6	3	PROMUS	2	39	4.2	0	25	0
7	3	Orsiro	0	64	0	0	112	0
8	4	BVS	16	52	18.4	3	57	1.2
9	4	BVS	11	51	17.9	0	71	0
10	4	CYPHER	68	24	64.9	0	76	0
11	5	BVS	4	83	4.4	–	–	–
12	5	BVS	23	92	19.9	–	–	–
13	6	BVS	25	80	20.1	–	–	–

Average% uncovered	Stent type	Week 1		Week 4	
		Average	SD	Average	SD
	PROMUS	6.6	2.1	0.0	0.0
	Orsiro	1.3	1.4	0.2	0.3
	CYPHER	48.4	23.3	0.0	0.0
	BVS	16.2	6.6	0.6	0.8

0.9 vs. 1.1, respectively) **(Figure 5C)**, as were the endothelialisation percentages for all (90.8% vs. 98% vs. 95.6% vs. 93.8%, respectively) **(Figure 5D)**. Histological analysis confirmed the delayed healing with absence of endothelium and tissue coverage at four weeks on NASB struts **(Figure 5, Figure 6)**.

COMPUTER SIMULATION

Simulation results describing shear rate and stress of a jailed side branch (struts) case are presented in **Figure 7** to show a representative difference in shear stress on a model stent across a side branch. Quantification results of spatial means of TAESS on the luminal

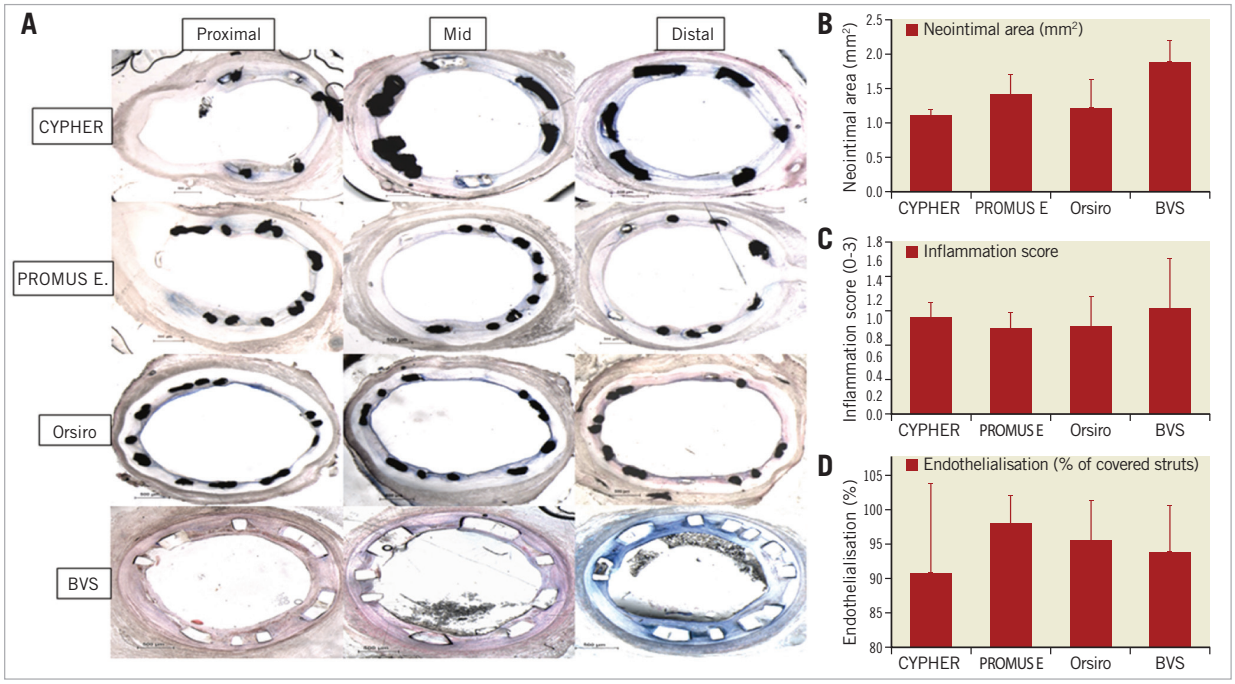

Figure 5. *Histological analysis at 4 weeks. A) Representative histologic images of struts organised according to stent type, vessel location and histology results according to stent type. B) Neointimal area. C) Inflammation score. D) Endothelialisation percentage observed.*

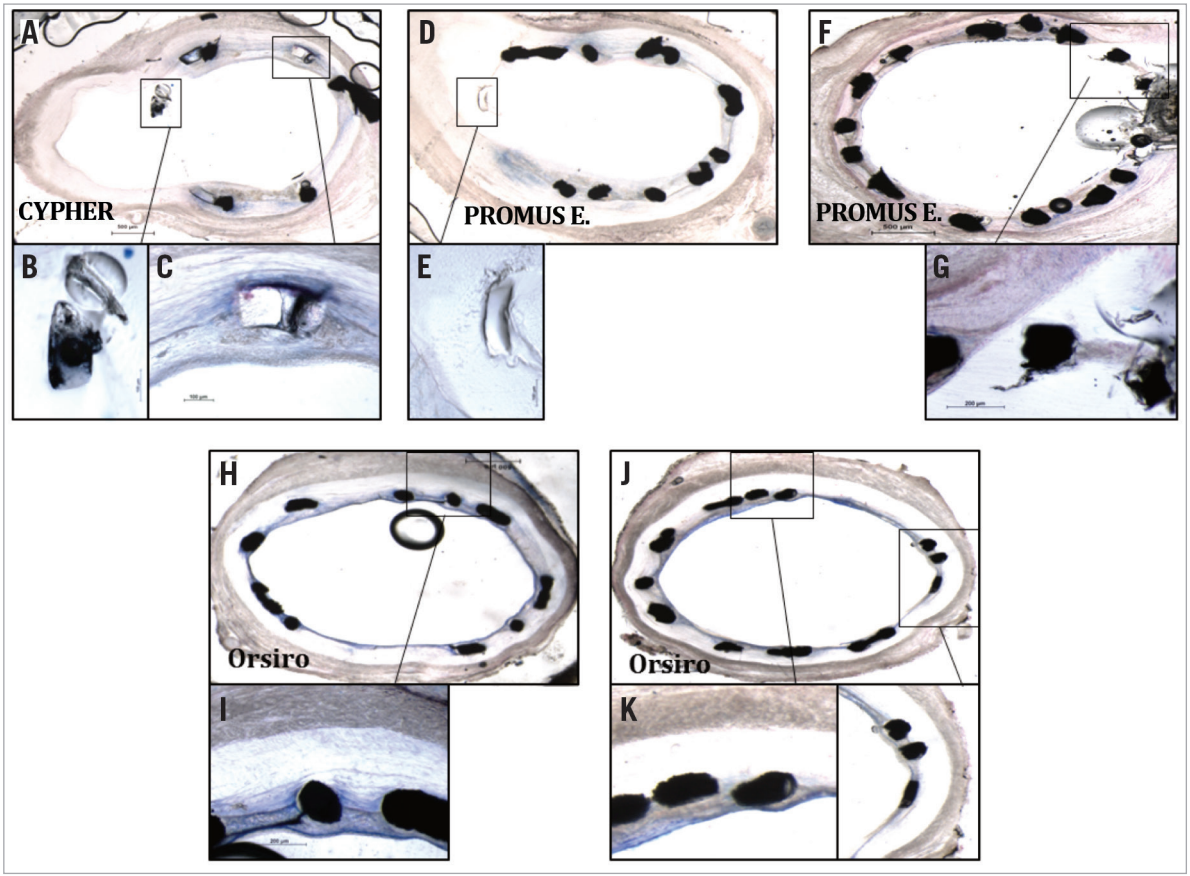

Figure 6. *Histologic images of uncovered struts at side branches of vessels. A) Histologic section: CYPHER stent in proximal LCX. High magnification images capturing uncovered strut in side branch (B) whereas apposed strut is well covered (C). D) & F) Histologic sections from region of LAD side branch containing PROMUS Element stent. E) & G) Note similar trend of struts floating in vicinity of side branch exhibiting minimal coverage. H) - K) Note the thin layer of neointimal tissue covering thin-strut Orsiro stent struts.*

side of the struts in the ostium compared with proximal and distal were 17.5 Pa, 4.2 Pa, and 5.4 Pa, respectively **(Figure 7)**.

Discussion

The main findings of this study are: 1) percentage of struts remaining uncovered at one week was lowest in the well-apposed segments followed by malapposed segments and highest in NASB struts (13.6%, 19.2% and 77.8%, respectively); 2) at four weeks, percentage of struts uncovered decreased in apposed and malapposed struts to 3.1% and 1.6% respectively, but 35.7% still in NASB struts; 3) neointimal coverage was thickest on apposed struts followed by malapposed struts and least on NASB struts. The impact of stent type was analysed in this study due to its implications in re-endothelialisation and the neointimal healing process. Endothelial coverage and the ratio of uncovered strut have been associated with stent thrombosis[5,11] and were selected as the parameters for analysis in this current study.

There are scarce data employing the use of sequential OCT to assess strut coverage coupled with implantation characteristics at different follow-up time points in patients, as such sequential assessment at more than two time points is difficult and only rarely available. Furthermore, using animals allowed us to study the coverage process in an *in vivo* model under controlled conditions. To the best of our knowledge, this is the first study to evaluate specifically with OCT the neointimal healing time course in relation to apposition and stent types. Most OCT-based studies exclude NASB struts from coverage analyses. Our results provide insights into the coverage of NASB struts by showing with OCT that only about 64.3% of NASB struts are covered one month after implantation in porcine models, confirming previous reports by other groups showing the delayed endothelialisation on NASB struts in patients[6,7,19].

The results of the current study suggest that coverage is fastest on the well-apposed segment. At one week, the percentage of struts covered in the well-apposed and ISA segments was 86.4% and 80.8%, respectively. Previous OCT studies in patients found the percentage of uncovered struts in well-apposed compared to malapposed struts to be 1% vs. 29%, respectively, at six-month follow-up ($p<0.01$)[16].

Furthermore, in our study, while the percentages of struts covered in well-apposed and ISA segments were essentially similar at four weeks (96.9% and 98.4%, respectively), the mean coverage thickness was higher in the well-apposed sections as compared with the ISA sections and NASB struts (0.12 mm vs. 0.11 mm

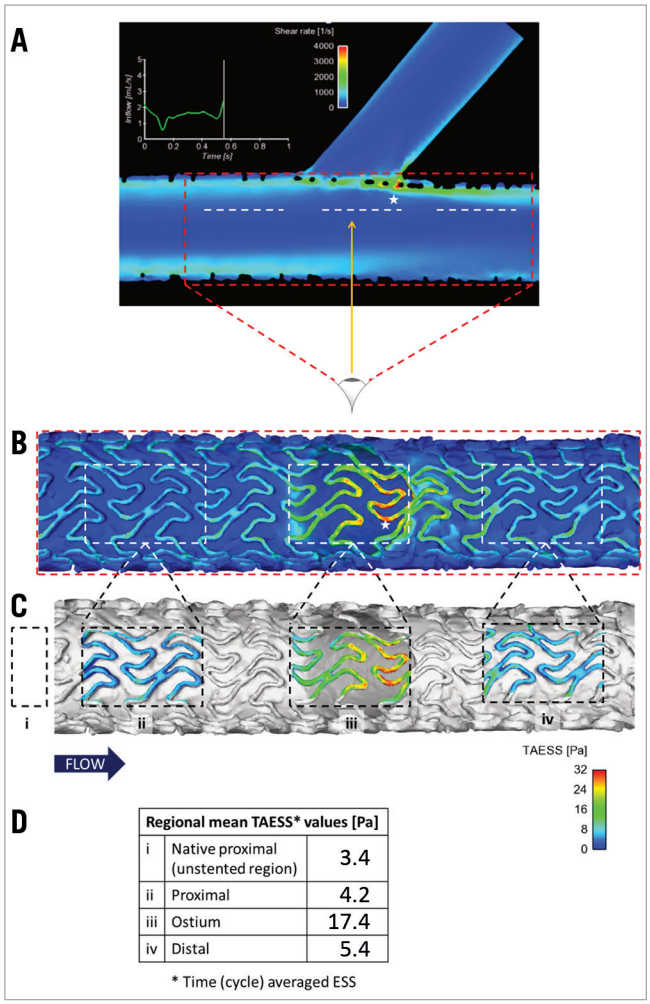

Figure 7. *Simulation results describing a shear rate and stress of jailed side branch (struts) case. A) Side view capturing the main branch and side branch. B) Bottom-top view of panel A (direction of arrow) capturing the cross-section of the ostium. Note that the white dashed boxes in panel B represent the cross-sectional views corresponding to the white dashed lines in panel A, and the stars indicate corresponding regions of high shear stress. Quantification results of spatial means of time (cycle) averaged endothelial shear stress (TAESS) on the luminal side of the struts in the ostium region (iii) as well as proximal (ii) and distal (iv) to the ostium are presented via colour-coded scheme in panel C and numerically in panel D. Reference value of shear stress from the native (unstented) part upstream (i) is also included.*

and 0.03 mm, respectively, $p<0.01$). The observations are probably attributable to the fact that coverage over time is dependent on detachment distance, as evidenced in previous OCT studies in patients[1,9].

There was, however, an interesting phenomenon observed in the current study. While previous OCT clinical studies have reported worse coverage in ISA struts compared with NASB struts[6], our results showed the opposite trend. This apparent contradiction is probably due to the fact that those studies involved atherosclerotic arteries where ISA was most likely the consequence of a more severely diseased vessel, with more severe calcification and poorer re-endothelialisation capabilities. In the current study, however, non-atherosclerotic animal models where shear-dependent neointimal tissue growth and re-endothelialisation are the main mechanisms, with ISA close to the healthy artery wall, leave NASB struts relatively disadvantaged. Shear stress levels are lower at close proximity to the vessel wall[20], and there exists an inverse relation between shear stress and neointimal hyperplasia[21], causing neointimal growth to be higher on the abluminal side of ISA struts[15]. Contrary to the abluminal side of the struts, however, the luminal side is subjected to high shear stress[15].

Consistent with the results on coverage, our analysis showed that, overall, the percentage of strut malapposition decreased over time **(Figure 2)**, as observed in previous clinical studies[10,22].

Studying stent coverage is important for providing insights into the fate of malapposed struts and the need for eventual optimisation to correct incomplete stent apposition. The results here suggest that well-apposed and thin struts represent the best situations to achieve fast coverage and re-endothelialisation. These are consistent with previous clinical and preclinical observations of coverage of ISA struts compared with well-apposed segments Our analysis of the impact of different strut designs also suggests that the neointimal coverage process is influenced by strut dimensions among other characteristics. At one week, only 1.3% of Orsiro struts (60 µm thickness) remained uncovered, while PROMUS Element, CYPHER and BVS, with larger strut thicknesses, had 6.6%, 48.4% and 16.2% of their struts still uncovered, respectively. Thinner struts produce smaller obstacles for the confluent endothelium layer and, as such, have faster integration into the vessel wall and re-endothelialisation than thicker struts[1,12,23].

The observed results are probably attributed but not limited to the fact that malapposed struts are subjected to different flow and shear stresses[1,20,23]. High shear forces present at bifurcations, as shown by the flow simulation results **(Figure 7)**, can explain the observation that NASB struts display the lowest extent of coverage in this study[6]. A relationship between shear stress and neointimal hyperplasia has been established in previous studies[1,15,21,23] but, to date, the precise physiological mechanism for this flow-dependent interaction still remains relatively unknown.

Study limitations

We recognise some limitations in our study, particularly the relatively low number of samples used for comparison.

While the present results suggest an effect of strut thickness on neointimal coverage and endothelialisation, it is important to note that the different polymer and drugs eluted corresponding to different stent designs are potentially also confounding factors contributing to the differences observed.

Although our study provides novel insights into the mechanism of coverage on struts, coverage is still used merely as a surrogate representation of complete vascular healing[2,3,11]. OCT imaging is currently unable to differentiate between types of coverage tissue,

fibrin, neointimal tissue or endothelium[3,11]. Also, the models used in this study were healthy young animals, and vascular healing response in diseased human patients' arteries is known to be comparatively slower than in porcine models.

Conclusions

Early neointimal response is influenced by stent apposition and stent strut characteristics. The results of this analysis show an important impact of baseline strut apposition on the risk of delayed strut coverage at follow-up. Insights provided by this study will help in the understanding of the mechanism of delayed coverage on malapposed segments and NASB struts and their evaluation by OCT.

Impact on daily practice

Previous clinical studies have associated stent malapposition and uncovered strut with adverse events (stent thrombosis). Neointimal response is influenced by apposition and stent strut design characteristics. The aim of this study was to evaluate by optical coherence tomography the impact of strut apposition and stent type on the progression of stent strut coverage in controlled *in vivo* models. The results of this analysis show that baseline strut apposition impacts on the risk of delayed strut coverage at follow-up, particularly for floating struts left unapposed in a bifurcation. Insights provided by this study will help in the understanding of the mechanism of coverage on well-apposed stent segments compared with malapposed segments and unapposed side branch struts.

Conflict of interest statement

This study was initiated and conducted independently by the authors. P. Wong and W. Shim are founders of Innoheart Plc (preclinical laboratory). I. Ang is an employee of Innoheart Plc. The other authors have no conflicts of interest to declare relevant to this study.

References

1. Foin N, Gutiérrez-Chico JL, Nakatani S, Torii R, Bourantas CV, Sen S, Nijjer S, Petraco R, Kousera C, Ghione M, Onuma Y, Garcia-Garcia HM, Francis DP, Wong P, Di Mario C, Davies JE, Serruys PW. Incomplete stent apposition causes high shear flow disturbances and delay in neointimal coverage as a function of strut to wall detachment distance: implications for the management of incomplete stent apposition. *Circ Cardiovasc Interv.* 2014;7:180-9.

2. Cook S, Eshtehardi P, Kalesan B, Raber L, Wenaweser P, Togni M, Moschovitis A, Vogel R, Seiler C, Eberli FR, Luscher T, Meier B, Jüni P, Windecker S. Impact of incomplete stent apposition on long-term clinical outcome after drug-eluting stent implantation. *Eur Heart J.* 2012;33:1334-43.

3. Gutierrez-Chico JL, Alegria-Barrero E, Teijeiro-Mestre R, Chan PH, Tsujioka H, de Silva R, Viceconte N, Lindsay A, Patterson T, Foin N, Akasaka T, Di Mario C. Optical coherence tomography: from research to practice. *Eur Heart J Cardiovasc Imaging.* 2012;13:370-84.

4. Foin N, Mattesini A, Ghione M, Dall'ara G, Sen S, Nijjer S, Petraco R, Sgueglia GA, Davies JE, Di Mario C. Tools & techniques clinical: optimising stenting strategy in bifurcation lesions with insights from in vitro bifurcation models. *EuroIntervention.* 2013;9:885-7.

5. Cook S, Ladich E, Nakazawa G, Eshtehardi P, Neidhart M, Vogel R, Togni M, Wenaweser P, Billinger M, Seiler C, Gay S, Meier B, Pichler WJ, Juni P, Virmani R, Windecker S. Correlation of intravascular ultrasound findings with histopathological analysis of thrombus aspirates in patients with very late drug-eluting stent thrombosis. *Circulation.* 2009;120:391-9.

6. Gutierrez-Chico JL, Regar E, Nüesch E, Okamura T, Wykrzykowska J, di Mario C, Windecker S, van Es GA, Gobbens P, Jüni P, Serruys PW. Delayed coverage in malapposed and side-branch struts with respect to well-apposed struts in drug-eluting stents: in vivo assessment with optical coherence tomography. *Circulation.* 2011;124:612-23.

7. Her AY, Kim JS, Kim YH, Shin DH, Kim BK, Ko YG, Choi D, Jang Y, Hong MK. Histopathologic validation of optical coherence tomography findings of non-apposed side-branch struts in porcine arteries. *J Invasive Cardiol.* 2013;25:364-6.

8. Sanchez OD, Yahagi K, Byrne RA, Mori H, Zarpak R, Wittchow E, Foin N, Virmani R, Joner M. Pathological aspects of bioresorbable stent implantation. *EuroIntervention.* 2015;11:V159-65.

9. Ozaki Y, Okumura M, Ismail TF, Naruse H, Hattori K, Kan S, Ishikawa M, Kawai T, Takagi Y, Ishii J, Prati F, Serruys PW. The fate of incomplete stent apposition with drug-eluting stents: an optical coherence tomography-based natural history study. *Eur Heart J.* 2010;31:1470-6.

10. Gutierrez-Chico JL, Wykrzykowska JJ, Nüesch E, van Geuns RJ, Koch KT, Koolen JJ, di Mario C, Windecker S, van Es GA, Gobbens P, Jüni P, Regar E, Serruys PW. Vascular tissue reaction to acute malapposition in human coronary arteries: sequential assessment with optical coherence tomography. *Circ Cardiovasc Interv.* 2012;5:20-9.

11. Finn AV, Joner M, Nakazawa G, Kolodgie F, Newell J, John MC, Gold HK, Virmani R. Pathological correlates of late drug-eluting stent thrombosis: strut coverage as a marker of endothelialization. *Circulation.* 2007;115:2435-41.

12. Joner M, Nakazawa G, Finn AV, Quee SC, Coleman L, Acampado E, Wilson PS, Skorija K, Cheng Q, Xu X, Gold HK, Kolodgie FD, Virmani R. Endothelial cell recovery between comparator polymer-based drug-eluting stents. *J Am Coll Cardiol.* 2008;52:333-42.

13. Finn AV, Nakazawa G, Joner M, Kolodgie FD, Mont EK, Gold HK, Virmani R. Vascular responses to drug eluting stents: importance of delayed healing. *Arterioscler Thromb Vasc Biol.* 2007;27:1500-10.

14. Foin N, Lee RD, Torii R, Guitierrez-Chico JL, Mattesini A, Nijjer S, Sen S, Petraco R, Davies JE, Di Mario C, Joner M,

Virmani R, Wong P. Impact of stent strut design in metallic stents and biodegradable scaffolds. *Int J Cardiol.* 2014;177:800-8.

15. Gutiérrez-Chico JL, Gijsen F, Regar E, Wentzel J, De Bruyne B, Thuesen L, Ormiston J, McClean DR, Windecker S, Chevalier B, Dudek D, Whitbourn R, Brugaletta S, Serruys PW. Differences in neointimal thickness between the adluminal and the abluminal sides of malapposed and side-branch struts: evidence in vivo about the abluminal healing process. *JACC Cardiovasc Interv.* 2012;5:428-35.

16. Gomez-Lara J, Radu M, Brugaletta S, Farooq V, Diletti R, Onuma Y, Windecker S, Thuesen L, McClean D, Koolen J, Whitbourn R, Dudek D, Smits PC, Regar E, Veldhof S, Rapoza R, Ormiston JA, Garcia-Garcia HM, Serruys PW. Serial analysis of the malapposed and uncovered struts of the new generation of everolimus-eluting bioresorbable scaffold with optical coherence tomography. *JACC Cardiovasc Interv.* 2011;4:992-1001.

17. Serruys PW, Onuma Y, Ormiston JA, de Bruyne B, Regar E, Dudek D, Thuesen L, Smits PC, Chevalier B, McClean D, Koolen J, Windecker S, Whitbourn R, Meredith I, Dorange C, Veldhof S, Miquel-Hebert K, Rapoza R, García-García HM. Evaluation of the second generation of a bioresorbable everolimus drug-eluting vascular scaffold for treatment of de novo coronary artery stenosis: six-month clinical and imaging outcomes. *Circulation.* 2010;122:2301-12.

18. Lingsma H, Nauta S, van Leeuwen N, Borsboom G, Bruining N, Steyerberg E. Tools & Techniques: Analysis of clustered data in interventional cardiology: current practice and methodological advice. *EuroIntervention.* 2013;9:162-4.

19. Nakazawa G, Yazdani SK, Finn AV, Vorpahl M, Kolodgie FD, Virmani R. Pathological findings at bifurcation lesions: the impact of flow distribution on atherosclerosis and arterial healing after stent implantation. *J Am Coll Cardiol.* 2010;55:1679-87.

20. Chen HY, Hermiller J, Sinha AK, Sturek M, Zhu L, Kassab GS. Effects of stent sizing on endothelial and vessel wall stress: potential mechanisms for in-stent restenosis. *J Appl Physiol (1985).* 2009;106:1686-91.

21. Wentzel JJ, Krams R, Schuurbiers JC, Oomen JA, Kloet J, van der Giessen WJ, Serruys PW, Slager CJ. Relationship between neointimal thickness and shear stress after Wallstent implantation in human coronary arteries. *Circulation.* 2001;103:1740-5.

22. Kim JS, Jang IK, Fan C, Kim TH, Kim JS, Park SM, Choi EY, Lee SH, Ko YG, Choi D, Hong MK, Jang Y. Evaluation in 3 months duration of neointimal coverage after zotarolimus-eluting stent implantation by optical coherence tomography: the ENDEAVOR OCT trial. *JACC Cardiovasc Interv.* 2009;2:1240-7.

23. Kolandaivelu K, Swaminathan R, Gibson WJ, Kolachalama VB, Nguyen-Ehrenreich KL, Giddings VL, Coleman L, Wong GK, Edelman ER. Stent thrombogenicity early in high-risk interventional settings is driven by stent design and deployment and protected by polymer-drug coatings. *Circulation.* 2011;123:1400-9.